Chapter 6
Microscopically Viewed Relationship Between Structure and Mechanical Property of Crystalline Polymers: An Important Guiding Principle for the Development of Super Fibers

Kohji Tashiro

Abstract The crystalline phase of polymer substance may be assumed as an idel state for the study of ultimate mechanical property of this polymer. The historical development in the study of structure-property relationship of polymer crystals has been reviewed by focusing on the crystallite modulus along the chain axis, the anisotropy in the lateral plane perpendicular to the chain axis, and the strength. This information is quite important as a guiding principle of the development of fibers with ultrahigh modulus and ultrahigh strength. In other words, the history of the development of these super fibers has been a challenge for approaching the goal of ultimate mechanical property. The experimental and theoretical methods to estimate the ultimate mechanical property of polymer crystals have been reviewed in Sects. 6.2, 6.3, 6.4, and 6.5. In the experimental approach, the X-ray diffraction peak shift and Raman band shift caused by the application of tensile stress are measured to detect the mechanical deformation of crystalline region, but the data analysis must be performed by taking the heterogeneous distribution into account. The quantum mechanical prediction of the ultimate strength of polymer chain has been reviewed in Sect. 6.6. The factors governing the strength of bulk polymer sample have been discussed concretely.

Keywords Young's modulus • Strength • Chain conformation • Crystal structure

K. Tashiro (✉)
Department of Future Industry-Oriented Basic Science and Materials, Toyota Technological Institute, Nagoya, Japan
e-mail: ktashiro@toyota-ti.ac.jp

6.1   Introduction

Historically viewed, the recognition of the possibility that the synthetic polymers possess the elastic modulus beyond the steel was made much earlier than the actual development of fibers with high Young's modulus and high strength. Let us see the case of polyethylene (PE). In 1949, Shimanouchi and Mizushima discovered the so-called accordion vibrational bands for a series of n-alkanes in the low-frequency region of Raman spectra [1]. The peak positions were found to shift inversely in proportion to the chain length. They interpreted these bands in terms of longitudinal acoustic vibration of a continuous body. This mode was found to correspond to the propagation of acoustic phonons in the polyethylene crystal along the chain axis [2]. In almost the same years, Lyons (1959) [3] and Treloar [4] calculated the Young's modulus of polyethylene zigzag chain on the basis of the theory about the balance of forces between the internal coordinates such as bond lengths and bond angles. Although the calculation was relatively rough, the theoretical evaluation of the Young's modulus of PE chain was made for the first time. In 1966, Odajima [5] calculated the elastic constants of orthorhombic polyethylene crystal on the basis of lattice dynamical theory developed by Born [6]. The vibrational frequency-phase angle dispersion curve of polyethylene crystal was calculated by Tasumi and Shimanouchi [7] and Krimm [8]. From the slope of the dispersion curve of the acoustic branch along the chain axis, the Young's modulus of polyethylene was estimated. In 1971, the neutron scattering measurement gave the dispersion curves experimentally and evaluated the Young's modulus as about 329 GPa [9]. On the other hand, in 1966, Sakurada et al. performed the X-ray diffraction measurement for the oriented polyethylene crystal under the constant tensile force, and the Young's modulus was estimated as 235 GPa, where the homogeneous stress distribution was assumed, i.e., the stress working on the crystal region was equal to the tensile stress in the bulk sample [10]. In the 1970s–1980s, the theoretical and experimental techniques to estimate the ultimate mechanical property of the various types of polymer crystals were developed remarkably [11]. In this way, it should be noticed that the prediction of the ultimate mechanical property of polymers was made in much earlier years before the development of actual polyethylene fiber with ultrahigh modulus in the 1980s.

   In the present article, the development of the molecular theoretical study on the relationship between structure and mechanical property of polymer materials in this half century is reviewed briefly, which has been an important guiding principle for the development of fibers of ultrahigh modulus and ultrahigh strength.

6.2   Experimental Evaluation of Ultimate Elastic Constants of Polymers

6.2.1   X-Ray Diffraction Method

Important mechanical property in the discussion of high-modulus fibers is the Young's modulus along the chain axis, which is named here the crystallite modulus E_c. Of course, the most ideal method for this purpose is to use a giant single crystal of polymer. The strain along the chain axis is estimated directly by applying a tensile force along the chain axis [12, 13]. Unfortunately, the usage of such a giant single crystal is limited at present to the polymers obtained by the photo-induced solid-state polymerization reaction, e.g., polydiacetylenes [12, 14] and poly (muconic ester) [13]. In the case of partially crystalline polymers, the X-ray diffraction method is one of the most excellent techniques [10]. The signal from the small crystallites is detected by measuring the X-ray diffractions. This point can be evaluated well in such a meaning that the mechanical property of small crystallites can be extracted even in the bulk sample consisting of the crystalline and amorphous regions. As pointed out in the introduction, this X-ray diffraction technique was accomplished by Sakurada et al. in the 1960s [10]. The small strain of the crystal is estimated by tracing the small shift of the X-ray diffraction peak corresponding to the lattice planes along the chain axis by applying a tensile force to the oriented sample. The shift of X-ray diffraction peak can be converted into the strain ε_c. Unfortunately, the stress σ_c working on the crystalline region cannot be known explicitly, and so it *must* be assumed to be equal to the macroscopic stress calculated from the actually applied tensile force and the cross-sectional area of the sample. This was named the assumption of homogeneous stress distribution. The E_c can be estimated as the initial slope in the $\sigma_c - \varepsilon_c$ curve, which is now termed as $E_c^{\text{X-ray}}$. For example, $E_c^{\text{X-ray}}$ is 235 GPa for polyethylene (PE) crystal, 40 GPa for *isotactic* polypropylene (*it*-PP) [15, 16], 53 GPa for polyoxymethylene (POM) [17], 100 GPa for poly(ethylene terephthalate) (PET) [18, 19], and so on.

As pointed above, these X-ray values were obtained under the assumption of homogeneous stress distribution. This assumption causes a serious problem in the evaluation of *true* Young's modulus of the crystalline region (E_c^{true}) in the semicrystalline polymer samples. In fact, in many cases, the E_c^{true} and $E_c^{\text{X-ray}}$ gave serious gap between them. For example, a giant single crystal of poly(muconic ester) of several centimeter lengths gives the E_c of 47 GPa, which was measured accurately by reading out the change in sample length under the application of tensile forces [13]. This value might be assumed as E_c^{true} in a good approximation. Luckily, this polymer can be melted and stretched to give the oriented semicrystalline samples. The crystallite modulus was estimated by the X-ray method under the assumption of homogeneous stress distribution. However, the $E_c^{\text{X-ray}}$ was only 17–35 GPa depending on the sample preparation conditions, far lower than the E_c^{true}. In this way, one of the most significant points about the X-ray diffraction method is that the $E_c^{\text{X-ray}}$ is not always common to all the samples, but it depends on

the preparation condition of the sample. This situation was found to occur also in the Raman scattering experiment, as will be mentioned in a later section. For the solution of this problem, Ward et al. [20] and Tashiro et al. [13, 21–23] utilized a complex mechanical model to show the heterogeneous stress distribution, which was proposed by Takayanagi et al. in 1963 [24]. The Young's modulus of the bulk sample (E_{bulk}) and E_c^{X-ray} (and Raman shift factor) were expressed in an explicit form on the basis of this mechanical model. The E_c^{true} was determined so that the observed data of E_{bulk} and E_c^{X-ray} (and Raman shift factor) were reproduced consistently. The above-mentioned relation of $E_c^{true} = 47$ GPa and $E_c^{X-ray} = 17$–35- GPa observed for poly(muconic ester) samples could be interpreted reasonably using this complex mechanical model [13]. This method was applied to the observed E_c^{X-ray} values of the various polymers, giving E_c^{true} of 75 GPa for POM (E_c^{X-ray} was 53–59 GPa for normally drawn samples and 72 GPa for ultra-drawn sample) [21], 260 ± 10 GPa for PE [21], and so on.

6.2.2   Vibrational Spectroscopic Method

In this way the correction of heterogeneous stress distribution gives in general a higher Young's modulus compared with E_c^{X-ray}. Such higher E_c values are detected in the vibrational spectroscopic experiments. As mentioned in the introduction, Shimanouchi and Mizushima discovered the accordion bands in the low-frequency region of Raman spectra of *n*-alkanes, which were interpreted reasonably using the longitudinal acoustic dispersion curve of polyethylene crystal along the chain axis [1, 2]. The evaluated Young's modulus was quite high, ca. 358 GPa. Strobl et al. [25] and Kobayashi et al. [26] corrected an effect of end-to-end interactions between the *n*-alkane molecules in the neighboring layers on the LAM (longitudinal acoustic mode) frequency and derived the E_c^{LAM} as 280–290 GPa, which is nearer to the E_c^{true}. The dispersion curve measured using coherent neutron scattering from the fully deuterated polyethylene crystal gave 329 GPa [9]. The theoretical calculation based on the lattice dynamical method gives 316 GPa [27]. For reference, the Young's modulus of ultra-drawn polyethylene fiber at low temperature was 288 GPa [28], which is closer to these spectroscopic values and far beyond the E_c^{X-ray}.

The Raman bands corresponding to the vibrational modes of the skeletal chains were shifted by applying the tensile force [29, 30]. In a small strain region, the shift is expressed as a linear function of stress ($\nu = -\alpha \cdot \sigma$). Similarly to the case of E_c^{X-ray}, the shift factor α is also affected sensitively by the morphology of the sample [21]. This fact is combined with the E_c^{X-ray} data to derive the heterogeneous stress distribution as already mentioned in the previous sections [13, 21–23].

6.3 Theoretical Evaluation of Ultimate Elastic Constants of Polymers

As mentioned in the introductory section, the theoretical estimation of E_c was performed already in the 1960s. The principle of the calculation was based on the static balance of forces between the internal coordinates such as bond lengths, bond angles, and torsional angles [3, 4, 31–34]. This method was developed by deriving the equation of E_c on the basis of lattice dynamical theory [5, 11, 31–36]. In this calculation the atomic displacements were expressed in terms of the accurate atomic coordinates and the reliable force constants, from which the three-dimensional elastic constants matrix can be derived. Odajima et al. calculated the elastic constant matrix of orthorhombic polyethylene crystal by the lattice dynamical theory for the first time [5]. Miyazawa et al. rewrote the equation by using matrices corresponding to the force constants and the atomic coordinates [35]. Tashiro et al. introduced the space group symmetry to the lattice dynamical equation and reduced the dimension of the giant matrices remarkably so as to accelerate the calculation rate of elastic constants, and they made it possible to apply the equation to any type of polymer crystal of complicated aggregation structure of atoms [36]. Another method is based on the molecular mechanics (MM), in which the potential energy of polymer chain (or polymer crystal) is numerically calculated by changing the repeating period along the chain axis step by step by considering the interactions between the atoms, from which the potential energy is expressed as a function of strain $(V = (1/2)E_c\varepsilon^2)$ and so the Young's modulus E_c is obtained as the second derivatives of potential energy V with respect to the strain ε [37]. The ab initio molecular orbital (MO) method is more sophisticated and calculates the potential energy based on Hamiltonian and a basis function set. The elastic constant matrix is obtained by the calculation of second derivatives of the thus calculated potential energy with respect to the Cartesian coordinates [38, 39]. These MM and MO methods give in general the overestimated values than the lattice dynamical method. In the latter case, the force constants between the internal displacement coordinates such as bond stretching, bond angle deformation, etc. were refined so that the calculated vibrational frequencies are in good agreement with the actually observed infrared and/or Raman spectra. The MM and MO give the relatively higher values to the vibrational frequencies. Sometimes the "adjustable parameter" was introduced in the MO calculation so that the thus-calculated frequencies were matched to the observed data.

The temperature dependence of the elastic constants can be estimated theoretically on the basis of molecular dynamics (MD) method [40–42]. The time-dependent fluctuation of potential energy of a crystal is calculated at the various temperatures, from which the elastic constant is obtained as a function of temperature.

6.4   Relationship Between Chain Conformation and Young's Modulus

As easily imagined, the Young's modulus E_c is sensitively dependent on the geometry or conformation of polymer chain and the interactions between the internal coordinates. More concretely, the E_c is expressed in an approximation as follows [11]:

$$1/E_c \propto \sum_i (\partial d/\partial R_i)^2/F_{ii} \propto \sum_i (\text{PED})_i$$

where $(\partial d/\partial R_i)$ is the first derivative of the pitch of one monomeric unit with respect to the internal coordinate R_i, F_{ii} is the diagonal term of force constant corresponding to R_i, and $(\text{PED})_i$ is the potential energy distribution to R_i. When a tensile force is applied along the chain axis, the potential energy is increased as a result of chain deformation, which is distributed to the various changes of the internal coordinates. This equation indicates that the E_c is related to the easiness of chain deformation $(\partial d/\partial R_i)$ and the rigidity of the change in R_i (F_{ii}) and that the internal coordinates having larger PED contribute to the determination of E_c. For example, Fig. 6.1 shows the deformation of molecular chains with the various PED values calculated for PE, PET, POM, PEOB (poly(ethylene oxybenzoate) α form), and PBO (poly-*p*-phenylene benzobisoxazole) [11, 42]. PE shows a high E_c because of its slim form and the PED to the skeletal C-C bond stretching and C-C-C angle deformation in almost equal percentage. PET chain is deformed by changing mainly the bond angles of ester carbon atoms (O-C(O)-benzene) so that the virtual bond passing through the benzene ring stands up toward the chain axis. Although PET chain possesses rigid benzene rings and ester groups, the E_c is not determined by the rigidity of these groups but by the easiness of deformation of zigzag angle. POM chain takes a helical form and the deformation occurs mainly through the change of COCO torsional angles as well as the change in bond angles (COC and OCO). POM shows relatively high E_c value because of the large contribution of bond angle deformation in addition to the torsional angle changes. PEOB α form takes a large zigzag conformation consisting of long arms and ethylene segmental parts. The chain deformation occurs mainly through the torsional motion around the ether bonds, giving quite low E_c of about 2 GPa. In the case of PBO, the whole of chain is so rigid, and the deformation occurs mainly through the stretching of linkages connecting the benzene and oxazole rings as well as the deformations of these rigid rings. The E_c value of 460 GPa is in the highest level among the various polymers.
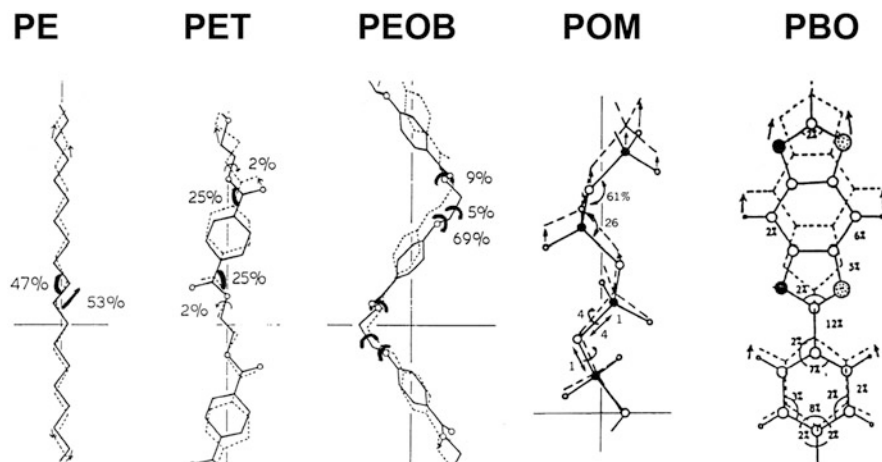
Fig. 6.1 Chain deformation and potential energy distribution calculated for the various polymers

6.5   Crystal Structure and Anisotropic Mechanical Property

The Young's modulus along the chain axis is one of the mechanical properties. The anisotropy in Young's modulus is also important in the discussion of the relationship between crystal structure and mechanical property [11]. The H...H intermolecular interactions in the crystal lattice govern mainly the anisotropy of the mechanical property. Therefore the Young's modulus in the lateral directions is one to two order lower compared with the modulus along the chain axis. Figure 6.2 shows the anisotropic curves of Young's modulus calculated for the various types of polymer crystals [11, 43]. In the case of orthorhombic PE crystal, the anisotropy is not very high, but the modulus is almost isotropic in the lateral directions because of the weak van der Waals forces between the hydrogen atoms. In the case of nylon 6, the sheet planes built up by hydrogen-bonded zigzag chains are stacked by weaker van der Waals interactions, resulting in the highly anisotropic mechanical property. These intermolecular interactions do not affect the Young's modulus along the chain axis very much. Poly-*p*-phenylene terephthalamide (PPTA) forms also the sheet structure similar to that of nylon 6 [44]. Therefore this polymer shows appreciably highly anisotropic mechanical property in the lateral direction as seen in Fig. 6.2. In the case of poly-*m*-phenylene isophthalamide (PMPI), the intermolecular hydrogen bonds are formed between the neighboring chains in a similar way as those of poly-*p*-phenylene terephthalamide, but when the direction of hydrogen bonds is viewed along the chain axis, it changes alternately perpendicularly along the *a* and *b* axes. As a result, the mechanical property is isotropically strong in the lateral directions [45]. POM chain takes a compact

Fig. 6.2 Anisotropic Young's modulus in the plane perpendicular to the chain axis calculated for the various types of polymer crystals (*PE* polyethylene, *PPTA* poly-*p*-phenylene terephthalamide, *PMPI* poly-*m*-phenylene isophthalamide), *POM* polyoxymethylene, and *PLLA* poly(L-lactic acid)
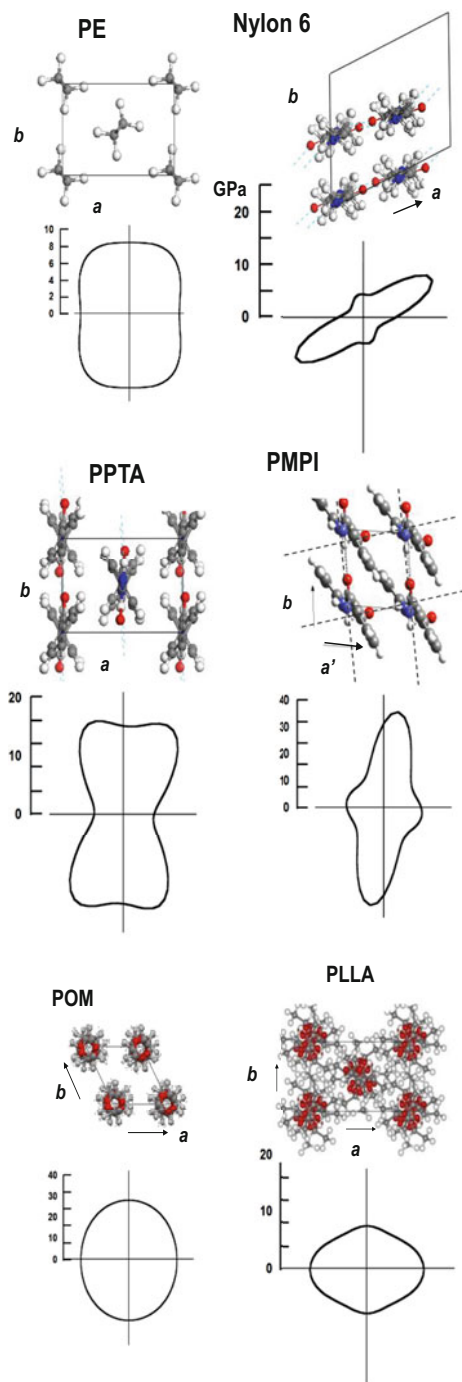
helical form, and these chains are closely packed in a hexagonal-type cell, resulting in the appreciably strong but isotropic Young's modulus in the lateral plane perpendicular to the chain axis [43]. Another typical example of helical chain conformation is observed for poly(L-lactic acid) [46]. The helices of large radius are packed in the crystal lattice in relatively loose manner, giving appreciably small and isotropic curve of the Young's modulus [43].

6.6   Strength of Polymer Chains

So far we have discussed the Young's modulus of polymer crystals or the mechanical property in the infinitesimally small deformation region. When the crystal is deformed in higher strain region, the crystal will be broken. The stress at this point is called the (fracture) strength. The fracture occurs by cutting the covalent bonds of the skeletal chain. If the potential energy of bond stretching mode is harmonic $(V = (1/2)E_c\varepsilon^2)$, the chain recovers to the original form necessarily even when the chain is stretched to a quite high strain. The breakdown of the covalent bond can be expressed using the anharmonic potential function, typical form of which is a so-called Morse potential function $\left(V = V_o\left(1 - e^{-k\Delta r}\right)^2\right)$. As the deformation $\Delta r \ (= r-r_o)$ becomes larger and reaches a certain value, then the potential energy reaches the flat value, where the recovery force becomes zero. This stress corresponds to the breakage stress. Since the breakage of covalent bond occurs by changing the electronic structure, more sophisticated method is based on the quantum mechanics. The repeating period along the chain axis is changed step by step, and the potential energy is calculated using a Hamiltonian operator. The recovery force is calculated as the first derivative of the potential energy. The recovery force reaches maximum and reduces sharply to zero at a certain strain, as shown in Fig. 6.3. The strength of PE chain was calculated to be about 45 GPa by the several researchers [47–49]. The sp^3 orbital of carbon atom changes to the sp^2 form when the radicals are generated at the ruptured C-C bond (see Fig. 6.3). However, the thus-estimated stress is too high compared with the actually observed strength of ultra-drawn PE sample, at most 6 GPa. The similar situation can be seen also for such rigid polymers as PBO [38].

These calculations did not consider the kinetic factor. As shown in Fig. 6.4, the scission of covalent bond is a chemical reaction. The system must cross the energy barrier E^* in the transition process from the bonded C-C bond to the fractured C atoms. When the stress σ is applied to the system, the barrier is reduced, and the probability to cross the barrier, expressed as $\exp[-(U - \beta\sigma)/kT]$, becomes higher, where k is the Boltzmann constant, T is an absolute temperature, and β is a proportional coefficient. Using this idea, the fracture strength was calculated by a Monte Carlo method, giving a few GPa, comparative to the realistic value [50–52].
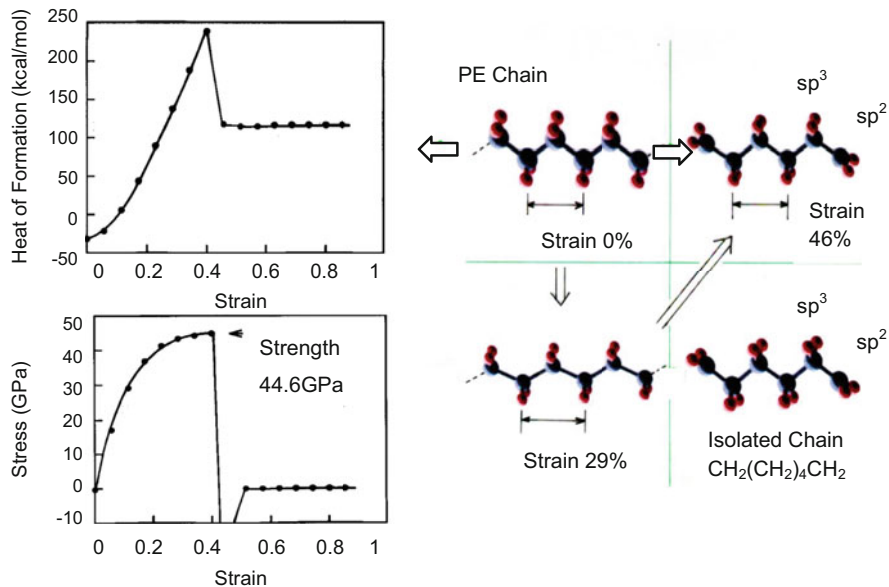
Fig. 6.3 Fracture of polyethylene zigzag chain calculated by quantum mechanical method: (**a**) the potential energy plotted against the strain, (**b**) the corresponding force, and (**c**) the chain deformation procedure
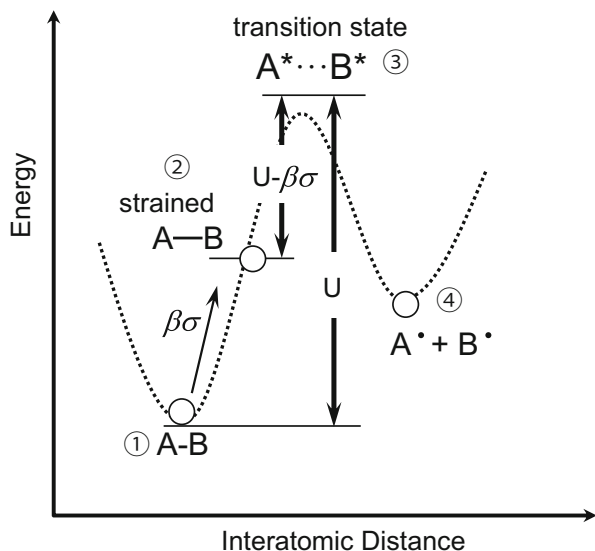

Fig. 6.4 Potential energy barrier in the A-B bond breakage process. (*1*) The original A-B bond, (*2*) the stretched A-B bond. The potential energy is increased by strain and (*3*) the barrier to cross the transient state A*...B* becomes lower. (*4*) The broken bond

In the actual case, the fracture of fibers does not only occur by the scission of C-C covalent bonds in the fully extended chains but also it occurs at the various structural defects through the separation of chains in the vicinity of chain ends, the slippage between the microfibrils, and so on. Because of these additional factors, the strength of a bulk sample becomes lower.

In this way the fracture of fibers must be interpreted by taking these various factors into consideration. Sometimes the phase transition might occur before the fracture, and the strength predicted must be changed correspondingly. Another factor important for the discussion of strength is the heterogeneous stress distribution. The local parts with structural defects might be damaged most easily if the stress concentration occurs there. One example is seen in carbon fiber (CF) [23, 53, 54]. The inner structure of a CF monofilament is not homogeneous but consists of the complicated aggregation of crystalline and amorphous regions. Roughly speaking, the CF monofilament takes a skin-core structure as revealed by the wide-angle X-ray scattering measurement using a synchrotron X-ray beam of micrometer size [53, 54]. The $E_c^{\text{X-ray}}$ and Raman shift factor (α) were found to be different depending on the CF monofilaments prepared at the different temperatures [53, 54]. The analysis was performed in a similar way using a complex mechanical model, from which the heterogeneous stress distribution was estimated in a quantitative manner. As shown in Fig. 6.5, the stress at the skin part is much higher than the core part. The skin part or the surface of CF monofilament is annealed at a higher temperature than the core part. As a result the Young's modulus of the surface part is higher and owes the stress at a higher level. The structure defect is said to generate relatively easily on the surface of CF monofilament, causing easier fracture of the CF starting from the surface part. In other words, the homogeneous heat treatment is needed for the production of the CF monofilament with homogeneous stress distribution. One idea is to use a microwave technique by which the PAN precursor is heated homogeneously to be a CF monofilament with higher modulus and higher strength than before [55].

Tie chain is also an important concept in the discussion of strength [56]. The tie chains pass through the neighboring lamellae and protect the stacked lamellae from the fracture. So far the tie chain had been assumed as only a hypothetical object. But one example is seen to show the actual existence of tie chains. This is a study of structural change in the isothermal crystallization of POM from the melt [57]. As well known, the infrared spectra of POM change sensitively depending on the morphology or the aggregation state of helical chains [58, 59]. The ECC (extended chain crystal) and FCC (folded chain crystal) can be distinguished by measuring the IR band characteristic of these morphologies. The time-dependent measurement of FTIR spectra during the isothermal crystallization from the melt revealed that the FCC bands appeared at first in parallel to the formation of the stacked lamellae as known from the small-angle X-ray scattering measurement. After that, the ECC bands started to appear, just when the daughter lamellae were generated between the mother lamellae, as shown in Fig. 6.6. The good correspondence between the appearance of ECC bands and daughter lamellae make it possible to imagine that the fully extended tie chain segments pass through the neighboring lamellae. When
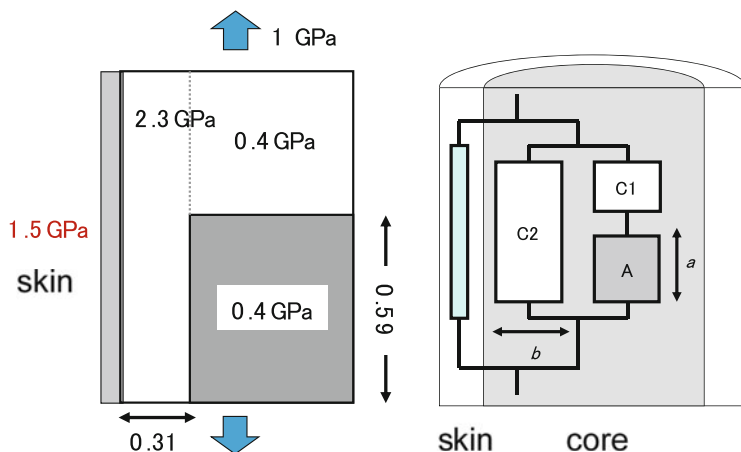
Fig. 6.5 The heterogeneous stress distributions calculated for the carbon fiber monofilament subjected to a tensile stress 1 GPa. The stress in the skin part is 1.5 times higher than the average stress
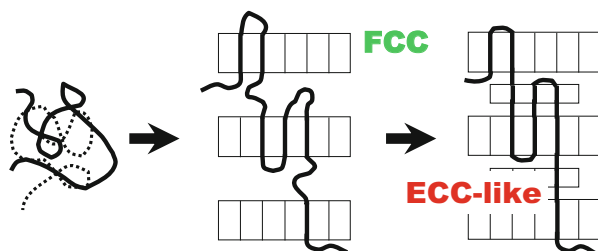

Fig. 6.6 Formation of tie chain segments in the melt-isothermal crystallization of polyoxymethylene

the POM sample is stretched, these tie chain segments may be tensioned and protect the fracture of stacked lamellae up to the critical stress causing the covalent bond breakage.

In this way the strength of bulk polymer material is governed by the various factors including the ultimate strength of fully extended chain, the kinetic effect of transient energy barrier, the structural defects, the slippage of microfibrils, the heterogeneous stress distribution, and the existence of taut tie chains. The theoretical estimation is still difficult at present for understanding the microscopically viewed correlation between the mechanical breakage and the chain aggregation state in the bulk polymer material by taking all of these factors into account.

References

1. S.I. Mizushima, T. Shimanouchi, J. Am. Chem. Soc. **71**, 1320 (1949)
2. R.F. Schaufele, T. Shimanouchi, J. Chem. Phys. **47**, 3605 (1967)
3. W.J. Lyons, J. Appl. Phys. **29**, 1429 (1958)
4. L.R.G. Treloar, Polymer **1**, 95 (1960)
5. A. Odajima, T. Maeda, J. Polym. Sci. Part C **15**, 55 (1966)
6. M. Born, K. Huang, *Dynamical Theory of Crystal Lattice* (Oxford University Press, London, 1954)
7. M. Tasumi, T. Shimanouchi, J. Chem. Phys. **43**, 1245 (1965)
8. M. Tasumi, S. Krimm, J. Chem. Phys. **46**, 755 (1967)
9. L. Holliday, J.W. White, Pure Appl. Chem. **26**, 545 (1971)
10. I. Sakurada, T. Ito, K. Nakamae, J. Polym. Sci. Part C **15**, 75 (1966)
11. K. Tashiro, Prog. Polym. Sci. **18**, 377–435 (1993)
12. G. Wu, K. Tashiro, M. Kobayashi, Macromolecules **22**, 188–196 (1989)
13. S. Nakamoto, K. Tashiro, A. Matsumoto, J. Polym. Sci. Part B Polym. Phys. **41**, 444–453 (2003)
14. G. Wegner, Pure Appl. Chem. **49**, 433 (1977)
15. K. Tashiro, M. Kobayashi, H. Tadokoro, Polym. J. **24**, 899–916 (1992)
16. C. Sawatari, M. Matsuo, Macromolecules **19**, 2653 (1986)
17. K. Nakamae, T. Nishino, K. Hata, T. Matsumoto, Kobunshi Ronbunshu **42**, 241 (1985)
18. M. Matsuo, C. Sawatari, Polym. J. **22**, 518 (1990)
19. T. Thistlethwaite, R. Jakeways, I.M. Ward, Polymer **29**, 61 (1988)
20. S. Jungnitz, R. Jakeways, I.M. Ward, Polymer **27**, 1651 (1986)
21. K. Tashiro, G. Wu, M. Kobayashi, Polymer **29**, 1768–1778 (1988)
22. T. Kitagawa, K. Tashiro, K. Yabuki, J. Polym. Sci. Part B Polym. Phys. **40**, 1281–1287 (2002)
23. T. Kobayashi, K. Sumiya, Y. Fujii, M. Fujie, T. Takahagi, K. Tashiro, Carbon **50**, 1163–1169 (2012)
24. M. Takayanagi, K. Imada, T. kajiyama, J. Polym. Sci. Part C Polym. Symp. **15**, 263 (1967)
25. G.R. Strobl, R. Eckel, J. Polym. Sci. Polym. Phys. Ed. **14**, 913 (1976)
26. M. Kobayashi, K. Sakagami, H. Tadokoro, J. Chem. Phys. **78**, 6391 (1983)
27. K. Tashiro, M. Kobayashi, H. Tadokoro, Macromolecules **11**, 914–918 (1978)
28. P.J. Barham, A. Keller, J. Polym. Sci. Polym. Lett. Ed. **17**, 591 (1979)
29. K. Tashiro, S. Minami, G. Wu, M. Kobayashi, J. Polym. Sci. Part B Polym. Phys. **30**, 1143–1155 (1992)
30. R.J. Young, R. Young, C. Ang, Strain Measurement in Fibres and Composites Using Raman Spectroscopy, Development in the Science and Technology of Composite Materials, Springer Netherlands, pp. 685–690 (1990).
31. T. Shimanouchi, M. Asahina, S. Enomoto, J. Polym. Sci. **59**, 93 (1962)
32. M. Asahina, S. Enomoto, J. Polym. Sci. **59**, 113 (1962)
33. H. Sugetam, T. Miyazawa, Polym. J. **1**, 226 (1970)
34. K. Tashiro, M. Kobayashi, H. Tadokoro, Macromolecules **10**, 731–736 (1977)
35. Y. Shiro, T. Miyazawa, Bull. Chem. Soc. Jpn. **44**, 2371 (1971)
36. K. Tashiro, M. Kobayashi, H. Tadokoro, Macromolecules **11**, 908–913 (1978)
37. G.C. Rutledge, U.W. Suter, Polymer **32**, 2179 (1991)
38. S.G. Wierschke, Mater. Res. Soc. Symp. **134**, 313 (1989)
39. J.R. Shoemaker, T. Horn, P.D. Haaland, R. Pachter, W.A. Adams, Polymer **33**, 3351 (1992)
40. J.R. Ray, Comp. Phys. Rep. **8**, 109 (1988)
41. K. Tashiro, Comp. Theor. Polym. Sci. **11**, 357–374 (2001)
42. K. Tashiro, M. Kobayashi, Macromolecules **24**, 306–3708 (1991)
43. K. Wasanasuk, K. Tashiro, Macromolecules **45**, 7019–7026 (2012)
44. K. Tashiro, M. Kobayashi, H. Tadokoro, Macromolecules **10**, 413–420 (1977)
45. K. Tashiro, M. Kobayashi, Polymer **32**, 1516–1526 (1991)

46. K. Wasanasuk, K. Tashiro, M. Hanesaka, T. Ohhara, K. Kurihara, R. Kuroki, T. Tamada, T. Ozeki, T. Kanamoto, Macromolecules **44**, 6441–6452 (2011)
47. D.S. Boudreaux, J. Polym. Sci. Polym. Phys. Ed. **11**, 1285 (1973)
48. B. Crist, M.A. Ratner, A.L. Brower, J.R. Sabin, J. Appl. Phys. **50**, 6047–6051 (2009)
49. K. Tashiro, J. Text. Mach. Soc. Jpn. **48**, 425 (1995)
50. Y. Termonia, P. Meakin, P. Smith, Macromolecules **19**, 154 (1986)
51. Y. Termonia, P. Smith, Macromolecules **20**, 835 (1987)
52. Y. Termonia, P. Smith, Macromolecules **21**, 2184 (1988)
53. T. Kobayashi, K. Sumiya, Y. Fukuba, M. Fujie, T. Takahagi, K. Tashiro, Carbon **49**, 1646–1652 (2011)
54. T. Kobayashi, K. Sumiya, Y. Fujii, M. Fujie, T. Takahagi, T. K., Carbon **53**, 29–37 (2013)
55. B.B. Balzer, J. McNabb, J. Ind. Tech. **24**, 1 (2008). http://atmae.org/jit/Articles/balzer061608.pdf
56. S.N. Zhurkov, V.E. Korsukov, J. Polym. Sci. Polym. Phys. Ed. **12**, 385 (1974)
57. H. Hama, K. Tashiro, Polymer **44**, 6973–6988 (2003)
58. M. Shimomura, M. Iguchi, Polymer **23**, 509 (1982)
59. M. Kobayashi, M. Sakashita, J. Chem. Phys. **96**, 748–760 (1992)